This article has been accepted and published on J-STAGE in advance of copyediting. Content is final as presented.

IEICE Electronics Express, Vol.VV, No.NN, 1–6

LETTER

Three-dimensional transmitter for omnidirectional wireless power transmission: design and experiment

Hao Qiang[1a)], Jiaqi Guan[1], Jianbo Wang[1], and Donghui Liu[1]

Abstract The omnidirectional wireless power transmission (WPT) technology have higher degree of freedom and less limitation in direction and space than the traditional WPT technology. This paper proposes a novel three-dimensional transmitter for omnidirectional wireless power transmission technology research. First, the magnetic field intensity distribution generated when three Tx coils are fed with different current phases is evaluated and analyzed. Then, the circuit topology of the system was analyzed and the mutual inductance between the transmitter (Tx) and receiver (Rx) coils was derived. Finally, an omnidirectional WPT experimental system was set up to validate all theoretical analyses.

key words: wireless power transmission, omnidirectional, three coils, magnetic fields

Classification: Energy harvesting devices, circuits and modules

1. Introduction

Research has shown that wireless power transmission (WPT) technology has excellent characteristics, such as high reliability, safety, flexibility, and so on[1]. Today WPT technology has been widely used, such as smart homes [2], electric vehicles [3, 4], the Internet of Things [5], industrial robotic [6, 7], implantable medical devices [8, 9], and underwater detection equipment [10, 11], and other fields.

In 2007, MIT proposed magnetically coupled resonant wireless power transfer (MCR-WPT) technology [12]. Compared with the existing WPT technologies, The MCR-WPT technology has the advantages of long transmission distance, high power, high efficiency, good directionality, and small environmental impact [13]. The traditional WPT system limits the location of the receiver, when there is a large offset between the magnetic couplers, which in turn will affect the transmission characteristics of the system [14, 15].

To solve the above problems, omnidirectional WPT technology was born, magnetically coupled transmitters under the control of multi-phase circuits can achieve uniform distribution of the magnetic field around the transmitter, which makes the omnidirectional WPT technology have higher degree of freedom and less limitation in direction and space than the traditional WPT technology. In [16], the mathematical analysis of the three-dimensional omnidirectional WPT system. The structure of the transmitter is an important strategy to achieve the uniformity of the magnetic field around the transmitter [17]. In [18, 19, 20], although the transmitter is a three-dimensional structure, it can only transmit power in two-dimensional direction and cannot achieve omnidirectional wireless power transmission. In [21], an Rx coil structure is proposed, to realize omnidirectional WPT with two-coil transmitter. In [22, 23, 24], the magnetic coupling transmitters are all two-dimensional planar structures. Although the dimension of the coil structure is reduced, multiple Rx coils are required to achieve omnidirectional power supply, increasing the complexity of the design. In[25], a receiver based on regular tetrahedron structure is proposed, but the receiver structure is complex. In [26], a bowl-mounted transmitter for charging portable devices is proposed, but due to the special structure of the coil, it is only suitable for specific occasions. In [27], a magnetic coupler with double three-dimensional coils is designed. However, the additional magnetic coupling between two three-dimensional coils increases the complexity of the system.

2. Coil structure design

2.1 Three-dimensional transmitter structure (topology)

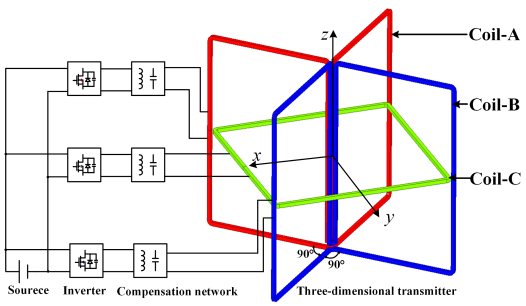


Fig. 1. Three-dimensional transmitter architecture for omnidirectional WPT system

In this paper, a novel three-dimensional transmitter for omnidirectional WPT systems is proposed, as shown in Fig.1. In Fig.1, the three-dimensional transmitter consists of Coil-A, Coil-B and Coil-C. Three inverters' circuits are adopted

[1]School of Mechanical Engineering and Rail Transit, Changzhou University, 213164, Changzhou, China
a) qhao@cczu.edu.cn

DOI: 10.1587/elex.20.20230561
Received November 23, 2023
Accepted December 18, 2023
Publicized December 25, 2023

Copyright © 2023 The Institute of Electronics, Information and Communication Engineers

to obtain alternating currents with different phases and fed into three coils to generate alternating magnetic field. The structure of Coil-A and Coil-B are folded and identical, as shown in Fig. 2(a).

Compared to square coil [28], Coil-A, Coil-B can generate better magnetic field, as shown in Fig. 2 (b). Furthermore, when two orthogonal coils are fed with currents of the same amplitude and phase, there is consistency between the direction of maximum magnetic field concentration and the direction of maximum power transmission, the magnetic field is concentrated on the angle bisector [29]. This characteristic can be achieved by independently exciting Coil-A, Coil-B.

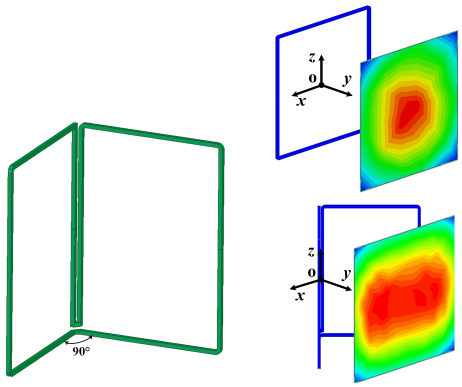


Fig. 2. (a) The shape of Coil-A and Coil-B, (b) Magnetic field distribution

2.2 Magnetic field analysis

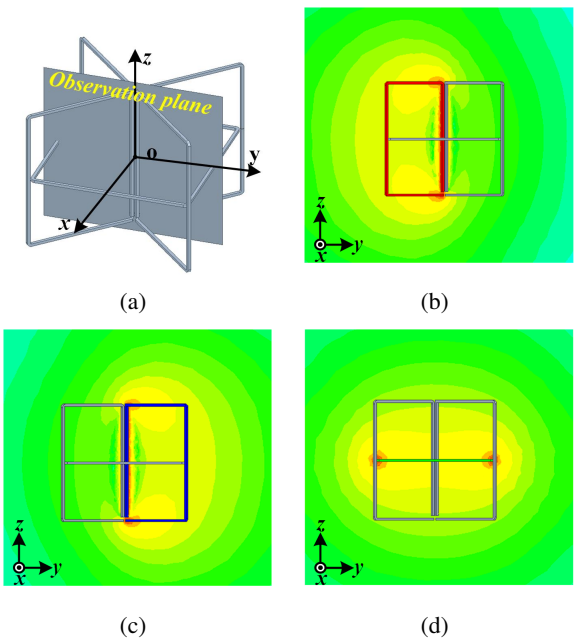


Fig. 3. Magnetic field distributions generated independently by Coil-A, Coil-B, and Coil-C. (a) Observation plane. (b) Coil-A. (c) Coil-B. (d) Coil-C

According to the actual structure of the transmitter, it is very difficult to establish a multi-turn transmitter simulation model in the simulation software to analyze the magnetic field distribution around the transmitter. However, in [22, 30] had proved that it is feasible and accurate to simplify the model and analyze the magnetic field by using single turn coils instead of multi turn coils. It should be noted that the model simplification is only used to analyze the magnetic field distribution around the transmitter and is not used to obtain the TX coil electrical parameters. This paper use ANSYS Maxwell to carry out the simulations in the frequency domain. The magnetic field generated by coils A, B, and C independently on the observation plane are shown in Fig. 3, and $x = 0$ (i.e. YOZ plane) is selected to be the observation plane. When only Coil-A is excited, the magnetic field is mainly distributed along the negative direction of y-axis, shown in Fig. 3(b). And it is distributed along the positive direction of y-axis when only Coil-B operates, shown in Fig. 3(c). When only Coil-C works, the magnetic field is mainly distributed along the z-axis, shown in Fig. 3(d).

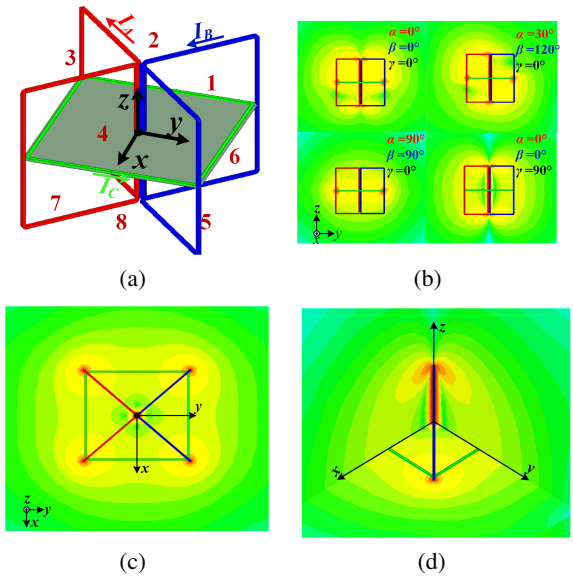
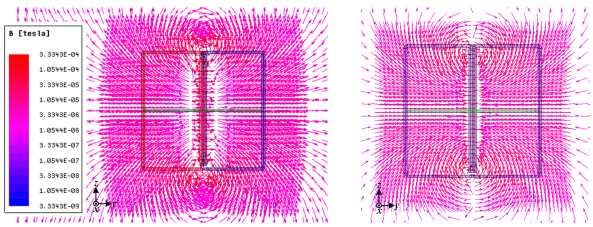


Fig. 4. (a) Quadrant division and current direction. (b) Magnetic field distribution of YOZ plane. (c) Magnetic field distribution of XOY plane. (d) 3D Magnetic field distributions for proposed three-dimensional Tx coils

Taking the geometric center of the three-dimensional transmitter structure as the origin, the entire space can be divided into eight quadrants based on the XYZ coordinates. The current directions in Coil-A, Coil-B and Coil-C are shown in Fig. 4(a). Analyze the magnetic field distribution in each quadrant under different current phase combinations.The phase combinations of currents I_A, I_B and I_C are exhaustively searched, where the excitation current vector in three coils is defined as $\dot{I}_A = \angle\alpha$, $\dot{I}_B = \angle\beta$ and $\dot{I}_C = \angle\gamma$, $\alpha, \beta, \gamma \in [0,\pi]$. Fig. 4(b) shows the magnetic field distribution of three Tx coils on the YOZ observation plane under several phase combinations when the amplitude of the excitation currents I_A, I_B and I_C fed into Coil-A, Coil-B and Coil-C

is 1A. When $\alpha = 0°$, $\beta = 0°$ and $\gamma = 90°$, Fig. 4(c) shows the magnetic field distribution on the XOY plane, Fig. 4(d) shows the three-dimensional magnetic field distribution of one top corner of the selected three-dimensional transmitter.

According to the magnetic field synthesis analysis and simulation results in [28], by adjusting currents in the three coils, it is impossible to simultaneously have large magnetic flux in quadrant 1 and 3 at the same time. In contrast, our transmitter can generate large magnetic fluxes in the 1 and 3 quadrants simultaneously with the corresponding control and it means that limitation on the position of the receiving coil has been reduced. From Fig. 4, when the current phases in Coil-A, Coil-B and Coil-C are 0°, 0° and 90°, the magnetic field distribution is evenly distributed in each region. Fig. 5 shows the magnetic vector-B distribution on the YOZ and XOZ plane, and the magnetic vector-B distribution is uniformly distributed in both observation planes. Clearly, our transmitter can create a more uniform magnetic field and can be used to simultaneously power supply to multiple receiving coils.



(a) (b)

Fig. 5. Magnetic vector-B distribution. (a) YOZ plane, (b) XOZ plane

3. Circuit model and characteristic analysis

3.1 System circuit model

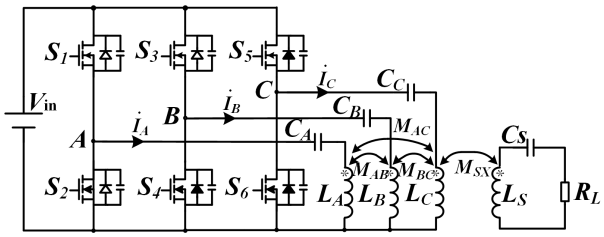


Fig. 6. Schematic of three-phase transmitter circuit with a receiver

To achieve omnidirectional WPT transmission, each Tx coil must be excited independently with different currents [29]. This paper adopts S-S resonance compensation topology, and the system equivalent circuit combined with the three-phase circuit is shown in Fig. 6. L_A, L_B, L_C and L_S represent self-inductance of three Tx coils and Rx coil, respectively. M_{AB}, M_{BC} and M_{AC} are the mutual inductances between three Tx coils. C_A, C_B, C_C and C_S the resonance compensation capacitances of three Tx coils and Rx coil. M_{SX} stands for the inductance between Coil-X and Coil-S, X= A, B, C. R_L is the load. Three inverter circuits are used to invert the DC voltage source into three alternating voltage sources, which are independently fed into the each Tx coil through a resonant compensation network. By tuning S_1-S_6, it is easy to obtain the ideal phase of the current in each Tx coil. The simplified mutual inductance equivalent circuit model as shown in Fig. 7.

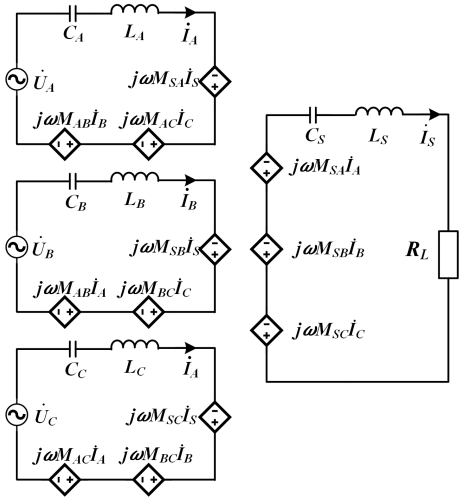


Fig. 7. Simplified mutual inductance equivalent circuit

In Fig. 7, $\dot{U}_A$, $\dot{U}_B$ and $\dot{U}_C$ stand for the high frequency AC power source. According to the simplified mutual inductance equivalent circuit model, the voltage KVL equation of the system with the operating angular frequency ω.

$$\begin{bmatrix} \dot{U}_A \\ \dot{U}_B \\ \dot{U}_C \end{bmatrix} = \begin{bmatrix} Z_A & j\omega M_{AB} & j\omega M_{AC} \\ j\omega M_{AB} & Z_B & j\omega M_{BC} \\ j\omega M_{AC} & j\omega M_{BC} & Z_C \end{bmatrix} \begin{bmatrix} \dot{I}_A \\ \dot{I}_B \\ \dot{I}_C \end{bmatrix} - \begin{bmatrix} j\omega M_{SA} \\ j\omega M_{SB} \\ j\omega M_{SC} \end{bmatrix} [\dot{I}_S] \tag{1}$$

$$0 = j\omega M_{SA}\dot{I}_A + j\omega M_{SB}\dot{I}_B + j\omega M_{SC}\dot{I}_C - Z_S\dot{I}_S \tag{2}$$

where, Z_A, Z_B, Z_C and Z_S are the equivalent impedances of the three Tx and Rx coils, $\dot{I}_A$,$\dot{I}_B$ and $\dot{I}_C$ and $\dot{I}_S$ are the currents input into the Tx and Rx coils, respectively. And ω it should be met.

$$\omega = \frac{1}{\sqrt{L_A C_A}} = \frac{1}{\sqrt{L_B C_B}} = \frac{1}{\sqrt{L_C C_C}} = \frac{1}{\sqrt{L_S C_S}} \tag{3}$$

Then

$$U = A \cdot I - B \cdot \dot{I}_S. \tag{4}$$

$$0 = B \cdot I - R_L \cdot \dot{I}_S. \tag{5}$$

where

$$U = \begin{bmatrix} \dot{U}_A & \dot{U}_B & \dot{U}_C \end{bmatrix}^T \tag{6}$$

$$A = \begin{bmatrix} Z_A & j\omega M_{AB} & j\omega M_{AC} \\ j\omega M_{AB} & Z_B & j\omega M_{BC} \\ j\omega M_{AC} & j\omega M_{BC} & Z_C \end{bmatrix} \tag{7}$$

$$I = \begin{bmatrix} \dot{I}_A & \dot{I}_B & \dot{I}_C \end{bmatrix}^T \tag{8}$$

$$B = \begin{bmatrix} j\omega M_{SA} & j\omega M_{SB} & j\omega M_{SC} \end{bmatrix}^T \tag{9}$$

Then, it can be solved as

$$I = (A - R_L B^T B)^{-1} U \tag{10}$$

$$\dot{I}_S = B(R_L A - B^T B)^{-1} U \tag{11}$$

$$P_{out} = R_e(R_L \cdot \dot{I}_S \cdot \dot{I}_S^*) \tag{12}$$

From the above equation, it can be seen that the load resistance, mutual inductance between the Tx and Rx coils, and three-phase input current are the main factors affecting the output characteristics of the WPT system.

3.2 Mutual inductance analysis

Fig. 8, shows the three-dimensional diagram for calculating the mutual inductance between the Tx and Rx coils. The range of θ is from 0 ° to 360 °. The shape of the coil and the distance between the coils are important factors affecting the mutual inductance between the Tx and Rx coils. In the proposed omnidirectional WPT system, all coils are polygons. Theoretically, the mutual inductance between any two coils can be obtained by summing the mutual inductance between the wires on each side of these two coils.

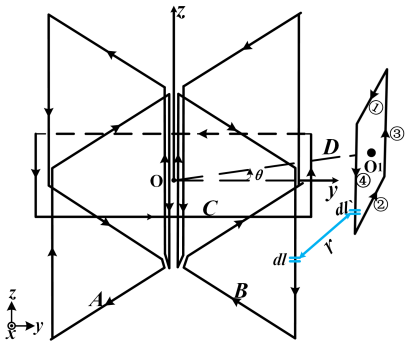


Fig. 8. Schematic diagram of mutual inductance calculation

Where, O and O_1 is the center of the three-dimensional transmitter and Rx coil. θ is the angle between the projection of the line $\overline{OO_1}$ on the XOY plane and y-axis. According to the Neumann formula, the mutual inductance M_{12} between two lines l_1 and l_2 can be expressed as

$$M_{12} = \frac{\mu_0}{4\pi} \int_{l_1} \int_{l_2} \frac{d\vec{l}_1 \cdot d\vec{l}_2}{r} \tag{13}$$

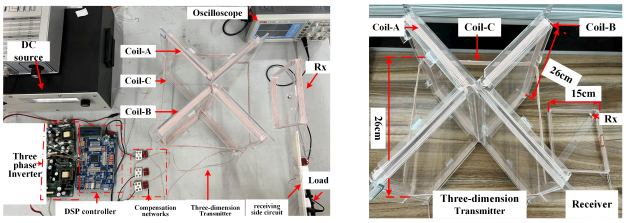
Where $d\vec{l}_1$ and $d\vec{l}_2$ stand for the infinitesimal micro vector elements and their distance is r. μ_0 is the vacuum permeability. It should be noted that when the currents in the line flow in the same direction, M_{12} is positive, otherwise it is negative. Then, the mutual inductance M between Coil-1 and Coil-2 can be deduced as

$$M = \sum_{i=1}^{K_1} \sum_{j=1}^{K_2} M_{ij} \tag{14}$$

Where, K_1 and K_1 represent the number of sides of the two coils.

4. Prototype and experimenta

In order to verify the previous theoretical analysis, the experimental platform of the proposed omnidirectional WPT system is shown in Fig. 9(a). The WPT system consists of DC voltage source, inverter circuit, DSP controller, resonant compensation network, three-dimensional transmitter, receiver, and load. Prototype of the constructed three-dimension transmitter and receiver is shown in Fig. 9(b). Litz wire with 0.05*250-strand is adopted to fabricate the coils. The system parameters of the experimental prototype are shown in Table I. The experiment utilizes LCR (meter TH2830) to measure the self-inductance, mutual inductance and resistance of coils, the oscilloscope is used to measure the voltage across the load.



(a) (b)

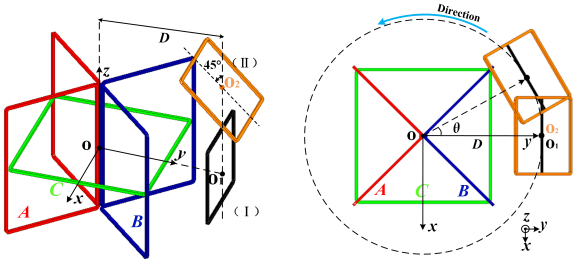
Fig. 9. (a) Experiment setup of proposed omnidirectional WPT system. (b) Prototype of the constructed three-dimension transmitter and receiver

Table I. Parameters of the prototype

Symbol	Value	Symbol	Value	Symbol	Value
L_A	96.3μH	f	85kHz	D	23cm
L_B	95.9μH	C_A	36.4nF	L_S	38.6μH
L_C	96.5μH	C_B	36.4nF	C_S	90.8nF
R_A	49.8mΩ	C_C	36.3nF	R_L	5Ω
R_B	50mΩ	R_C	51mΩ	R_S	23mΩ
N_A,N_B	10	N_C	11	N_S	10

4.1 Measurement and analysis of mutual inductance

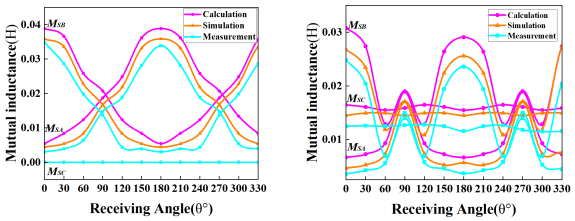
When the Rx coil is rotated around the three-dimensional transmitter, the mutual inductance is obviously changed. Fig. 10 shows the two various rotating case while D is fixed. In



(a) (b)

Fig. 10. (a) Stereogram of coil configuration. (b) Planform of coil configuration

Case-I, the Rx coil is perpendicular to XOY plane and O_1 is on XOY plane. And in Case-II, the positions of O_2 is (x,y,13cm), and the angle between the Rx coil and z-axis is 45°. The theoretical value, simulation value and measured value of M_{SX} are shown in Fig. 11.



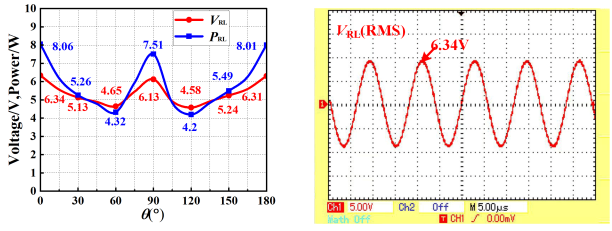
(a) (b)

Fig. 11. Theoretical value, simulation value and measured value of M_{SX}. (a) Case-I, (b) Case-II

In Fig. 11, the theoretical value is basically consistent with simulation value. And due to manual winding and measurement deviation, the measured value is low than the theoretical value and simulation value. The Msx changes symmetrically about θ = 180°. In Case-I and Case-II, M_{SA} and M_{SB} reach the maximum values when θ = 180 ° and θ = 0 °, respectively. M_{SC} changes little with θ.

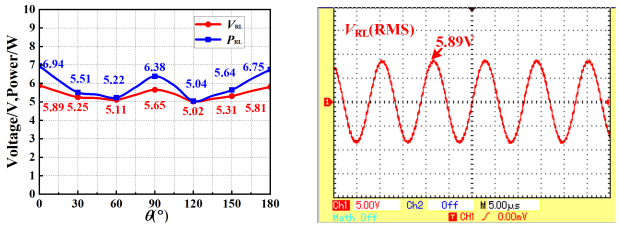
4.2 Experimental analysis

According to the above analysis, When α = 0°, β = 0° and γ = 90°, respectively. In Case-I and Case-II, the load voltage V_{RL} and power P_{RL} are various with θ, as shown in Fig. 14 and Fig. 15. Due to the symmetry of three-dimensional transmitter, the actual measurement range of θ is from 0° to 180°.



(a) (b)

Fig. 12. Case-I. (a) Trend of V_{RL} and P_{RL} varying with angle θ. (b) Waveform of the voltage V_{RL} with angle θ = 0°



(a) (b)

Fig. 13. Case-II. (a) Trend of V_{RL} and P_{RL} varying with angle θ. (b) Waveform of the voltage V_{RL} with angle θ = 0°

In Fig. 12(a), when θ = 0° and θ = 180°, O_1 is on the x-axis, V_{RL} and V_{RL} are the maximum, which are 6.34V/8.06W and 6.31V/8.01W. When θ = 90°, M_{SA} and M_{SB} are almost equal, and the V_{RL}L and P_{RL} are close to the maximum. When θ = 60° and θ= 120°, V_{RL} and P_{RL} are the minimum, which are 4.32V/4.65W, 4.2V/4.58W, respectively. When θ= 0°, the waveform of V_{RL} is shown in Fig. 12(b).

In Fig. 13(a), when θ changes from 0° to 180°, the range of V_{RL} and P_{RL} are 5.02V-5.89V and 5.04W-6.94W, respectively. Compared to Case-I, V_{RL} and P_{RL} fluctuate less with θ and are more uniformly distributed. When θ = 0°, the waveform of V_{RL} is shown in Fig. 13(b).

In practical applications, the Tx coil and the Rx coil may not be completely aligned, and there may be a certain angle misalignment φ, as shown in Fig. 14. When φ changes from 0° to 90°, V_{RL} decreases continuously, and when φ = 90°, V_{RL} is almost equal to 0V.

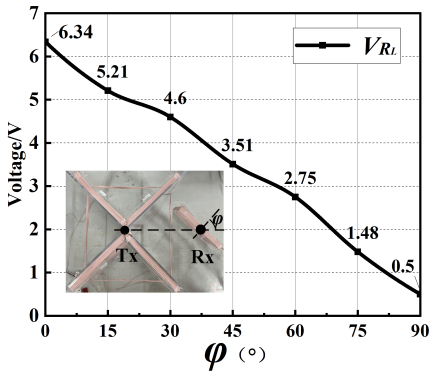


Fig. 14. Trend of voltage V_{RL} varying with misalignment angle φ

When the input power is 10 W, the maximum efficiency is 80.6% when θ = 0° in Case-I. Because of the presence of Coil-C, the minimum efficiency of 42% is also occued in Case-I. The experimental results show that for the proposed three-dimensional transmitter not only utilizes the characteristics of orthogonal coils that can transmit maximum power in a specific direction, but also realizes the omnidirectional wireless power transmission.

5. Conclusion

For achieving the omnidirectional wireless power transmission, this paper designs a novel three-dimensional transmitter based on three Tx coils. By ANSYS Maxwell, the magnetic field distribution of this transmitter has been evaluated when three Tx coils are fed with currents of different phases, and a strong uniform omnidirectional magnetic field distribution can be obtained. Then based on the principle of equivalent circuits, the transmission performance and mutual inductance of the omnidirectional wireless transmission system are analyzed. Finaly, an 85 kHz omnidirectional wireless power transmission system prototype is designed to carry out experiments. And the experimental results show

that the proposed three-dimensional transmitter has the ability of omnidirectional power transmission. When the Rx coil is in the two rotational cases of Case-I and Case-I, the transmission efficiency varies between 42%-80.6% and 50.4%-69.4% respectively. However, when supplying power to multiple receiving coils simultaneously, how to adjust the current phase control strategy in Tx to reduce the coupling effect between these receiving coils will be one goal of our future work.

References

[1] H. Guo, et al.: "Overview of Research and Application of Space Omnidirectional Radio Energy Transmission Technology," Chinese Journal of Electrical Engineering **47** (2012) 2898 (DOI: 10.1109/ISSCC.2012.6177094).

[2] W. Li: "Detailed Description and Design of Inductive Wireless Charging Products," Collection (2019) 124 (DOI: 10.19514/j.cnki.cn32-1628/tm.2019.27.067).

[3] Z. Wang, et al.: "Research Progress in Wireless Charging Technology for Electric Vehicles," Journal of Power Supply (2014) 27 (DOI: 10.13234/j.issn.2095-2805.2014.3.27).

[4] D. Patil, et al.: "Wireless Power Transfer for Vehicular Applications: Overview and Challenges," IEEE Trans. Transp. Electrific **4** (2018) 3 (DOI: 10.1109/TTE.2017.2780627).

[5] W. Na, et al.: "Energy-Efficient Mobile Charging for Wireless Power Transfer in Internet of Things Networks," IEEE Internet Things **5** (2018) 79 (DOI: 10.1109/JIOT.2017.2772318).

[6] J. Wu, et al.: "A Coupling Mechanism With Multi-degree Freedom for Bidirectional Multistage WPT System," IEEE Trans. Power Electron **36** (2021) 1376 (DOI: 10.1109/TPEL.2020.3010955).

[7] Md. R, et al.: "Stable and High-Efficiency Wireless Power Transfer System for Robotic Capsule Using a Modified Helmholtz Coil," IEEE Trans. Ind. Electron **64** (2017) 1113 (DOI: 10.1109/TIE.2016.2614268).

[8] B. Lee, et al.: "A Triple-Loop Inductive Power Transmission System for Biomedical Applications," IEEE Trans. Biomed. Circuits Syst **10** (2016) 138 (DOI: 10.1109/TBCAS.2014.2376965).

[9] J. S. Ho, et al.: "Midfield Wireless Powering for Implantable Systems," Chinese Journal of Electrical Engineering **101**(2013) 1369 (DOI: 10.1109/JPROC.2013.2251851).

[10] X. Wu, et al.: "Overview of Underwater Radio Energy Transmission Technology and Application Research," Journal of Electrical Technology **34** (2019) 1559 (DOI: 10.19595/j.cnki.1000-6753.tces.180691).

[11] Z. Yan, et al.: "A Rotation-Free Wireless Power Transfer System With Stable Output Power and Efficiency for Autonomous Underwater Vehicles," IEEE Trans. Power Electron **34** (2019) 4005 (DOI: 10.1109/TPEL.2018.2871316).

[12] A. Kurs, et al.: "Wireless Power Transfer via Strongly Coupled Magnetic Resonances," Science **317** (2007) 83 (DOI: 10.1126/science.1143254).

[13] X. Huang, et al.: "Research Trends and Application Prospects of Magnetic Coupling Resonant Radio Energy Transmission Technology," Power System Automation **41** (2017) 2.

[14] S. Y. Choi, et al.: "Asymmetric Coil Sets for Wireless Stationary EV Chargers With Large Lateral Tolerance by Dominant Field Analysis," IEEE Trans. Power Electron **29** (2014) 6406 (DOI: 10.1109/TPEL.2014.2305172).

[15] J. Zhang, et al.: "Comparative Analysis of Two-Coil and Three-Coil Structures for Wireless Power Transfer," IEEE Trans. Power Electron **32** (2017) 341 (DOI: 10.1109/TPEL.2016.2526780).

[16] D. Lin, et al.: "Mathematic Analysis of Omnidirectional Wireless Power Transfer—Part-II Three-Dimensional Systems," IEEE Trans. Power Electron **32** (2017) 613 (DOI: doi: 10.1109/TPEL.2016.2523506).

[17] C. Rong, et al.: "Omnidirectional Free-Degree Wireless Power Transfer System Based on Magnetic Dipole Coils for Multiple Receivers," IEEE Access **9** (2021) 81588 (DOI: doi: 10.1109/ACCESS.2021.3085307).

[18] N. H. Van and C. Seo: "Analytical and Experimental Investigations of Omnidirectional Wireless Power Transfer Using a Cubic Transmitter," IEEE Trans. Ind Electron **65** (2018) 1358 (DOI: 10.1109/TIE.2017.2733470).

[19] F. Liu, et al.: "Parametric Optimization of a Three-Phase MCR WPT System With Cylinder-Shaped Coils Oriented by Soft-Switching Range and Stable Output Power, " IEEE Trans. Power Electron **35** (2020) 1036 (DOI: 10.1109/TPEL.2019.2914154).

[20] L. Tan, et al.: "Power Stability Optimization Design of Three-Dimensional Wireless Power Transmission System in Multi-Load Application Scenarios," IEEE Access **8** (2020) 91843 (DOI: 10.1109/ACCESS.2020.2994653).

[21] J. H. Kim, et al.: "Plane-Type Receiving Coil With Minimum Number of Coils for Omnidirectional Wireless Power Transfer," IEEE Trans. Power Electron **35** (2020) 6165 (DOI: 10.1109/TPEL.2019.2952907).

[22] B. H. Choi, et al.: "Six Degrees of Freedom Mobile Inductive Power Transfer by Crossed Dipole Tx and Rx Coils," IEEE Trans. Power Electron **31** (2016) 3252 (DOI: 10.1109/TPEL.2015.2449290).

[23] T. Feng, et al.: "A Reticulated Planar Transmitter Using a Three-Dimensional Rotating Magnetic Field for Free-Positioning Omnidirectional Wireless Power Transfer," IEEE Trans. Power Electron **37** (2022) 9999 (DOI: 10.1109/TPEL.2022.3155251).

[24] T. Feng, et al.: "A Tripolar Plane-Type Transmitter for Three-Dimensional Omnidirectional Wireless Power Transfer," IEEE Trans. on Ind. Applicat **58** (2022) 1254 (DOI: 10.1109/TIA.2021.3107471).

[25] X. Dai, et al.: "A Novel Multi-Degree Freedom Power Pickup Mechanism for Inductively Coupled Power Transfer System," IEEE Trans. Magn **53** (2017) 1 (DOI: 10.1109/TMAG.2016.2550523).

[26] J. Feng, et al.: "Transmitter Coils Design for Free-Positioning Omnidirectional Wireless Power Transfer System," IEEE Trans. Ind. Inf **15** (2019) 4656 (DOI: 10.1109/TII.2019.2908217).

[27] W. Han, et al.: "Design and Analysis of Quasi-Omnidirectional Dynamic Wireless Power Transfer for Fly-and-Charge," IEEE Trans. Magn **55** (2019) 1 (DOI: 10.1109/TMAG.2019.2895716).

[28] Q. Zhu, et al.: "Field Orientation Based on Current Amplitude and Phase Angle Control for Wireless Power Transfer," IEEE Trans. Ind. Electron **65** (2018) 4758 (DOI: 10.1109/TIE.2017.2767556).

[29] W. M. Ng, et al.: "Two- and Three-Dimensional Omnidirectional Wireless Power Transfer," IEEE Trans. Power Electron **29** (2014) 4470 (DOI: 10.1109/TPEL.2014.2300866).

[30] C. Park, et al.: "Innovative 5-m-Off-Distance Inductive Power Transfer Systems With Optimally Shaped Dipole Coils," IEEE Trans. Power Electron **30** (2015) 817 (DOI: 10.1109/TPEL.2014.2310232).